Full text open access online (Since 2001)
© IJHG 2022
PRINT: ISSN 0972-3757 ONLINE: ISSN 2456-6330

Int J Hum Genet, 22(3): 173-184 (2022)
DOI: 10.31901/24566330.2022/22.03.803

Roles of Long Non-coding Ribonucleic Acid X Inactive Specific Transcript/microRNA-29a/phosphatase and Tensin Homolog Deleted on Chromosome Ten Pathway in Osteogenic Differentiation of Bone Marrow Mesenchymal Stem Cells and Postmenopausal Osteoporosis

Bin Wu[1], Binfeng Jiang[2], Jin Wang[2] and Jian Liu[2,*]

[1]Department of Orthopedics, the Second Affiliated Hospital of Jiaxing University, Jiaxing 314 000, Zhejiang Province, China
[2]Department of Orthopedics, Tongde Hospital of Zhejiang Province, Hangzhou 310 012, Zhejiang Province, China

KEYWORDS Bone Marrow Mesenchymal Stem Cell, Long Non-coding Ribonucleic Acid, MicroRNA, Postmenopausal Osteoporosis

ABSTRACT The researchers aimed to inquire into the roles of long non-coding ribonucleic acid X inactive specific transcript/microRNA-29a/phosphatase and tensin homolog deleted on chromosome ten (lncRNA-XIST/miR-29a/PTEN) pathway in the osteogenic differentiation of bone marrow mesenchymal stem cells (BMSCs) and postmenopausal osteoporosis (PMOP). In the miR-29a + Lenti-NC group, ALP activity, concentration of alizarin red, and mRNA and protein expressions of Runx2, OPN and OCN significantly increased, whereas the mRNA and protein expressions of LPL, AP-2 and leptin decreased ($P<0.05$). In contrast with the miR-29a + Lenti-NC group, miR-29a + Lenti-XIST and miR-29a + Lenti-PTEN groups had decreased ALP activity, concentration of alizarin red, and mRNA and protein expressions of Runx2, OPN and OCN, but increased mRNA and protein expressions of LPL, AP-2 and leptin ($P<0.05$). BMSCs have incremental expressions of lncRNA-XIST and PTEN and a declined expression of miR-29a. LncRNA-XIST suppresses the osteogenic differentiation of BMSCs by feat of the miR-29a/PTEN pathway.

INTRODUCTION

Postmenopausal osteoporosis (PMOP) is defined as bone metabolism disorders put down to superior bone resorption to bone formation due to ovarian function decline and insufficient estrogen secretion (Söreskog et al. 2021). The disease is primarily manifested as ostealgia and fractures, and frequently occurs in middle-aged and elderly postmenopausal women, seriously affecting patients' physical and mental health and quality of life (Baccaro et al. 2015). As members of the mesenchymal stem cell family, bone marrow mesenchymal stem cells (BMSCs) are able to differentiate into adipocytes, osteocytes and chondrocytes, and stimulate osteocalcin (OCN) release in osteoclasts, thereby facilitating bone growth and remodeling (Zhou et al. 2019; Zhong et al. 2020). The differentiation of BMSCs into adipocytes and osteocytes may be a significant pathogenesis of PMOP (Wang et al. 2021; Zhang et al. 2021).

*Address for correspondence:
Jian Liu
E-mail: liujianthzp@ltyz-edu.cn

Long non-coding ribonucleic acids (lncRNAs) and microRNAs (miRNAs) play key roles in osteoblast differentiation (Sun et al. 2021; Lin et al. 2021). X inactive specific transcript (XIST) exhibits significantly downward content in the differentiation of synovial mesenchymal stem cells into chondrocytes, and silencing XIST expression promotes such differentiation (Zhu et al. 2021). Moreover, the down-regulation of lncRNA-XIST can enhance the proliferation and differentiation of osteoblasts upon rheumatoid arthritis, as a treatment target (Wang et al. 2020). MiR-29a-3p promotes the differentiation of BMSCs into osteocytes in a high-fat environment (Luo et al. 2019). Moreover, research implemented by Xu et al. (2020) manifested that in the case of PMOP, the expression of miR-29a-3p waned, and cartilage degeneration occurred. Additionally, Alsina et al. (2018) found that phosphatase and tensin homolog deleted on chromosome ten (PTEN) inhibited bone morphogenetic protein 9 (BMP9)-induced activity of alkaline phosphatase (ALP) in C3H10T1/2 mouse embryonic fibroblasts, and

suppressed the expression and mineralization of early and late osteogenic markers. However, whether lncRNA-XIST, miR-29a and PTEN are associated with one another in the differentiation of BMSCs into osteocytes has been rarely reported. It has previously been described that PMOP displayed a close correlation with the endogenous expressions of lncRNA-XIST, miR-29a and PTEN (Ghafouri-Fard et al. 2021).

Objectives

An ovariectomized rat model was established, and the expressions and variations of the lncRNA-XIST/miR-29a/PTEN pathway during the differentiation of BMSCs into osteocytes were analyzed, aiming to explore the molecular mechanism of PMOP.

MATERIAL AND METHODS

Material

Laboratory animals were SPF female SD rats purchased from SINO ANIMAL (Beijing) Co., Ltd. (China; license No. SYXK (Beijing) 2020-0051).

The main reagents and apparatus included miR-negative control (NC) and miR-29a (Guangzhou RiboBio Co., Ltd., China), Lenti-NC, Lenti-XIST and Lenti-PTEN (Shanghai HanBio Co., Ltd., China), α-minimum essential medium (α-MEM), ALP staining kit and alizarin red S staining kit (Shanghai Beyotime Biotechnology Co., Ltd., China), Runt-related transcription factor 2 (Runx2), OCN and osteopontin (OPN) antibodies (CST, USA), horseradish peroxidase-labeled secondary antibodies (Beijing Bersee Science and Technology Co., Ltd., China), lipoprotein lipase (LPL), adipocyte binding protein-2 (AP-2) and leptin antibodies (Shenzhen Otwo Biotech Co., Ltd., China), bicinchoninic acid (BCA) protein concentration assay kit (Beijing Zhongshan Golden Bridge Biotechnology Co., Ltd., China), refrigerated centrifuge (Beckman Coulter, USA), protein electrophoresis and membrane transfer apparatus (Bio-Rad, USA), and electron microscope (Olympus, Japan).

PMOP Modeling and Grouping

Twenty female SD rats were randomly divided into a Sham group (n=10) and an ovariectomy group (PMOP group, n=10). After intraperitoneal injection of 3 percent sodium pentobarbital (40 mg/kg) for anesthetizing the rats, the abdomen was longitudinally cut open layer by layer along the midline, bilateral ovaries were found and removed by silk ligation, and then the incision was sutured layer by layer. For the Sham group, only the exposure of the ovaries was implemented, without removal of the ovaries. Penicillin (100,000 U/d) was intraperitoneally injected for 3 consecutive days following surgery. After routine feed for 8 weeks, ascertainment of the bone mineral density (BMD) was executed on the right femur. The modeling was considered successful if significantly waned BMD was ascertained in the PMOP group in contrast to the Sham group ($P<0.05$).

Culture and Identification of BMSCs

BMSC isolation and cultivation were done. To be specific, after the rats were sacrificed, the unilateral femur and tibia were aseptically isolated, and the amputation of metaphysis at both ends was executed. Afterwards, α-MEM incorporating 10 percent fetal bovine serum was employed to quickly wash the bone marrow cavity. Thereafter, the washing solution was collected, pipetted several times and centrifuged, followed by casting aside of the supernatant. Next, resuspension of the solution was done with α-MEM incorporating 10 percent fetal bovine serum, followed by culture in a 5 percent CO_2 incubator at 37°C, with replacement of the medium every 48 h. Following the cell density hit 80-90 percent, cell trypsinization and passage were executed, and the third (P3)-generation BMSCs were harvested for further experiments.

For osteogenic differentiation, the osteogenic induction solution was added into the P3-generation BMSCs for inducing differentiation. 3 weeks later, the BMSCs were dyed with alizarin red, and the mineralized nodules were observed under an optical microscope (×100).

For adipogenic differentiation, the P3-generation BMSCs were induced to differentiate with adipogenic induction solution. Next, the BMSC were dyed with oil red O after the lipid droplets became large and round enough, followed by watching of the staining results under the optical microscope (×100).

To identify the surface markers of BMSCs, the P3-generation of BMSCs were added PE-labeled cluster of differentiation (CD) 90 and CD44, APC-labeled CD45 and FITC-labeled CD31, respectively, and the expressions of corresponding antigens were ascertained by flow cytometry.

Transfection and Grouping

According to the instructions of Lipofectamine™2000, transfection of BMSCs was executed with miR-NC and miR-29a, respectively, during which the culture medium was replaced with lentiviral-pEF-1a/Puro-NC (Lenti-NC), lentiviral-pEF-1a/Puro-XIST (Lenti-XIST) and lentiviral-pEF-1a/Puro-PTEN (Lenti-PTEN) fresh medium containing 6 mg/L polybrene with a multiplicity of infection of 20. Afterwards, 48 h of BMSC cultivation was done at 37°C in the 5 percent CO_2 incubator .

The BMSCs were allocated to miR-NC + Lenti-NC, miR-NC + Lenti-XIST, miR-29a + Lenti-NC, miR-29a + Lenti-XIST, miR-NC + Lenti-PTEN and miR-29a + Lenti-PTEN groups.

Detection of Targeted Binding of lncRNA-XIST to miR-29a and of miR-29a to PTEN by Luciferase Assay

The targeted binding sites of XIST to miR-29a and those of miR-29a to PTEN were anticipated based on miRcode (http://www.miRcode.org) and TargetScanHuman (http://www.targetscan.org/vert_72/), respectively, showing that XIST and PTEN may be the target genes of miR-29a. Then construction of XIST and PTEN wild-type 3' untranslated region (3'UTR) vectors (XIST-WT, PTEN-WT) and mutant 3'UTR luciferase reporter vectors (XIST-MUT, PTEN-WT) was conducted, followed by mixing with miR-NC and miR-29a in the order given, and co-transfection into BMSCs by Lipofectamine™2000 for 48 h. Thereafter, the BMSCs were harvested and prepared into cell lysate, and ascertainment of the luciferase activity was executed in accordance with the kit's instructions to determine whether miR-34a bound XIST and PTEN 3'UTR.

ALP Staining

Following inoculating transfected BMSCs into a 24-well plate, culture in calcium salt medium was implemented for 7 d. Next, washing with PBS 3 times, and fixation with 4 percent paraformaldehyde at room temperature for 20 min were accomplished. After casting aside paraformaldehyde, NBT/ALP solution was added for ALP staining in dark for 30 min, and the staining results were observed. Blue outlines in the cytoplasm indicated that ALP in cells bound the dye. In diethanolamine buffer (pH 9.8, 37°C), the amount of ALP required to produce 1 ìmol p-nitrophenol from p-nitrophenyl phosphate chromogenic substrate hydrolyzed per minute was defined as an ALP activity unit. The ALP activity in the sample was figured up based on the definition of enzyme activity.

Alizarin Red S Staining

After the inoculation of transfected BMSCs into a 24-well plate, the BMSCs were cultivated in calcium salt medium for 14 d. Afterwards, BMSC washing and fixation were executed separately with PBS (3 times) and 4 percent paraformaldehyde (at room temperature for 20 min). After casting aside paraformaldehyde, 0.4 percent alizarin red S was added for staining, the reaction was terminated with deionized water, and the calcium deposition was observed under the microscope. Dark red calcified nodules outside the alizarin red-stained cells indicated calcium production. Then reading of the absorbance at 405 nm was executed exercising a microplate reader according to the instructions of alizarin red staining kit. The alizarin red standard curve was plotted, and the concentration in sample was calculated.

Detection of mRNA Expressions of lncRNA-XIST, miR-29a and PTEN, Osteogenic Markers OCN, OPN, Runx2 and Adipogenic Markers LPL, AP-2 and Leptin in BMSCs by qRT-PCR

TRIzol was adopted for total RNA extraction from BMSCs, followed by reverse transcription into cDNA. Next, amplification was accomplished using SYBR Green, with GAPDH as the internal reference under the undermentioned reaction conditions: pre-denaturation at 95°C for 5 min, 95°C for 10 s, and 62°C for 30 s, a total of 40 cycles. Thereafter, the computation of relative mRNA expression levels of Runx2, OPN and OCN

was executed by $2^{-\Delta\Delta CT}$. PCR primer sequences were as follows: XIST-F: 5'-ACGCTGCATGTGTC-CTTAG-3', XIST-R: 5'-GAGCCTCTTATAGCT-GTTTG-3'. PTEN-F: 5'-TAGTGACAATGAACCT-GATCA-3', PTEN-R: 5'-GGTAATCTGACA-CAATGTCCTA-3'. Runx2-F: 5'-GCACTAC-CCAGCCACCTTTA-3', Runx2-R: 5'-TATGGAGT-GCTGCTGGTCTG-3'. OPN-F: 5'-GAGCAAACA-GACGATGTGGA-3', OPN-R: 5'-GACCAGCT-CATCGGATTCAT-3'. OCN-F: 5'-TCACACTGCT-TGCCCTACTG-3', OCN-R: 5'-TGCCATA-GAAGCGCCGATAG-3'. LPL-F: 5'-TTGCTATTC-CAGGGTATCCA-3', LPL-R: 5'-TGTTAGTTGT-TGTCCCATCG-3'. AP-2-F: 5'-TCCTGCACCAC-CAACTGCTTAG-3', AP-2-R: 5'-AGTGGCAGT-GATGGCATGGACT-3'. Leptin-F: 5'-CCAGGAT-GACACCAAAACCC-3', Leptin-R: 5'-TATCTG-CAGCACGTTTTGGG-3'. GAPDH-F: 5'-GGT-GAAGGTCGGAGTGAACG-3', GAPDH-R: 5'-CGTGGGTGGAATCATACTGGA-3'.

Detection of Protein Expressions of lncRNA-XIST, PTEN, Osteogenic Markers OCN, OPN and Runx2 and Adipogenic Markers LPL, AP-2 and Leptin in BMSCs by Western Blotting

Total protein extraction was conducted by adding an appropriate amount of RIPA lysis buffer to part of BMSCs, followed by ascertainment of the protein concentration using BCA kit. After dilution with buffer, the protein was subjected to SDS-PAGE for separation, followed by quick transfer of the products onto a PVDF membrane. Then the membrane was subjected to 2 h of blocking in tris-buffered saline incorporating Tween 20 (TBST) with 5 percent skim milk at room temperature, and incubation with XIST, PTEN, Runx2, OPN, OCN, LPL, AP-2 and leptin primary antibodies (dilution ratio: 1:2000) through the whole night at 4°C . Thereafter, membrane washing was executed with TBST for 3 times, followed by incubation of the membrane again with secondary antibodies (dilution ratio: 1:10,000) at indoor temperature for 2 h. Finally, the color was developed with ECL reagent in dark. The gray values of protein bands were recorded and photographed using Bio-Rad gel imager. GAPDH served as the control, and quantitative analysis of protein expression was executed.

Statistical Analysis

SPSS16.0 software was employed for statistical analysis. The measurement data were described as mean ± standard deviation ($\bar{x} \pm s$) and compared between two groups by the *t* test. $P<0.05$ was considered to be statistically significant.

RESULTS

Morphological Observation and Identification of BMSCs

The P3-generation BMSCs in Sham and PMOP groups were closely arranged in a vortex shape, exhibiting a long spindle shape with the same morphology (Fig. 1A). After osteogenic induction, the cells turned from long spindle shape to short spindle and square shapes, the cell colonies were distributed in layers, calcium deposition gradually emerged in BMSCs, and red dense nodules were discerned, but the Sham group exhibited a larger area of red nodules than that the PMOP group (Fig. 1B). After adipogenic induction, BMSCs gradually became round from long spindle, the intracellular lipid droplets continuously increased, fused and became larger, and the lipid droplets were red, but a larger number of lipid droplets was watched in the PMOP group in contrast to the Sham group (Fig. 1C). In terms of the surface markers of BMSCs, CD90 and CD44 were positively expressed (Sham group: 99.8 percent and 99.5 percent, PMOP group: 99.5 percent and 99.8 percent), while CD45 and CD31 were negatively expressed (Sham group: 0.40 percent and 0.004 percent, PMOP group: 0.42 percent and 0.005 percent) (Fig. 1D). Taken together, the adherent cells isolated from the bone marrow of SD rats were BMSCs. The BMSCs in the Sham group underwent osteogenic differentiation, while those in the PMOP group were subjected to adipogenic differentiation.

mRNA Expression Levels of lncRNA-XIST, miR-29a, PTEN, Osteogenic Markers Runx2, OPN and OCN and Adipogenic Markers LPL, AP-2 and Leptin during Osteogenic Differentiation of BMSCs

In Sham and PMOP groups, significantly rose mRNA expression levels of miR-29a and osteo-

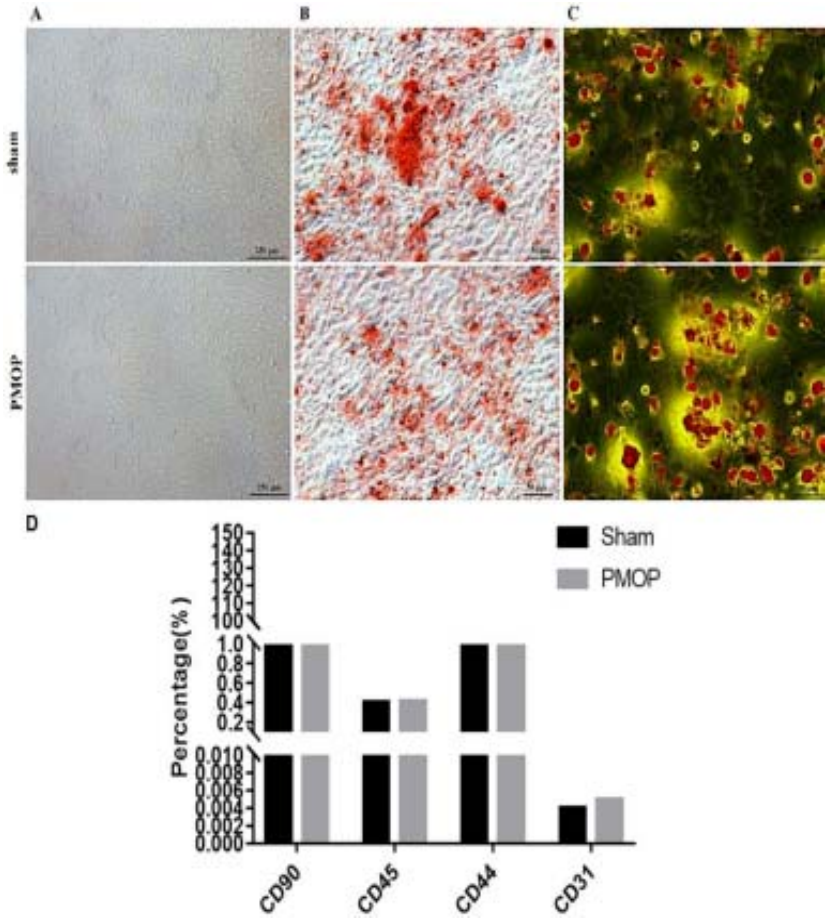

Fig. 1. Morphological observation and identification of BMSCs. A) P3-generation BMSCs; B) alizarin red staining; C) oil red O staining; D) identification of surface markers of BMSCs

genic markers (Runx2, OPN and OCN) were noticed at 7, 14 and 21 d after osteogenic induction compared with those at 0 d, and the Sham group displayed higher mRNA expression levels of such indexes than the PMOP group ($P<0.05$). Additionally, Sham and PMOP groups manifested the significantly downward mRNA expression levels of lncRNA-XIST and PTEN and adipogenic markers LPL, AP-2 and leptin, and these levels were lower in the Sham group than those in the PMOP group ($P<0.05$). Differentiation into osteocytes and adipocytes was inversely proportional to the extension of culture time. The differentiation of BMSCs into osteocytes and adipocytes was severally noted in the Sham group and PMOP group (Fig. 2).

Targeted Regulatory Relationships among lncRNA-XIST, miR-29a and PTEN

According to forecasting by starBase, miR-29a was a potential downstream target of lncRNA-XIST (Fig. 3A). Based on TargetScanHuman, PTEN was screened out as the target gene of miR-29a, and the two had binding sites in 3'UTR (Fig. 3C). In accordance with luciferase reporter

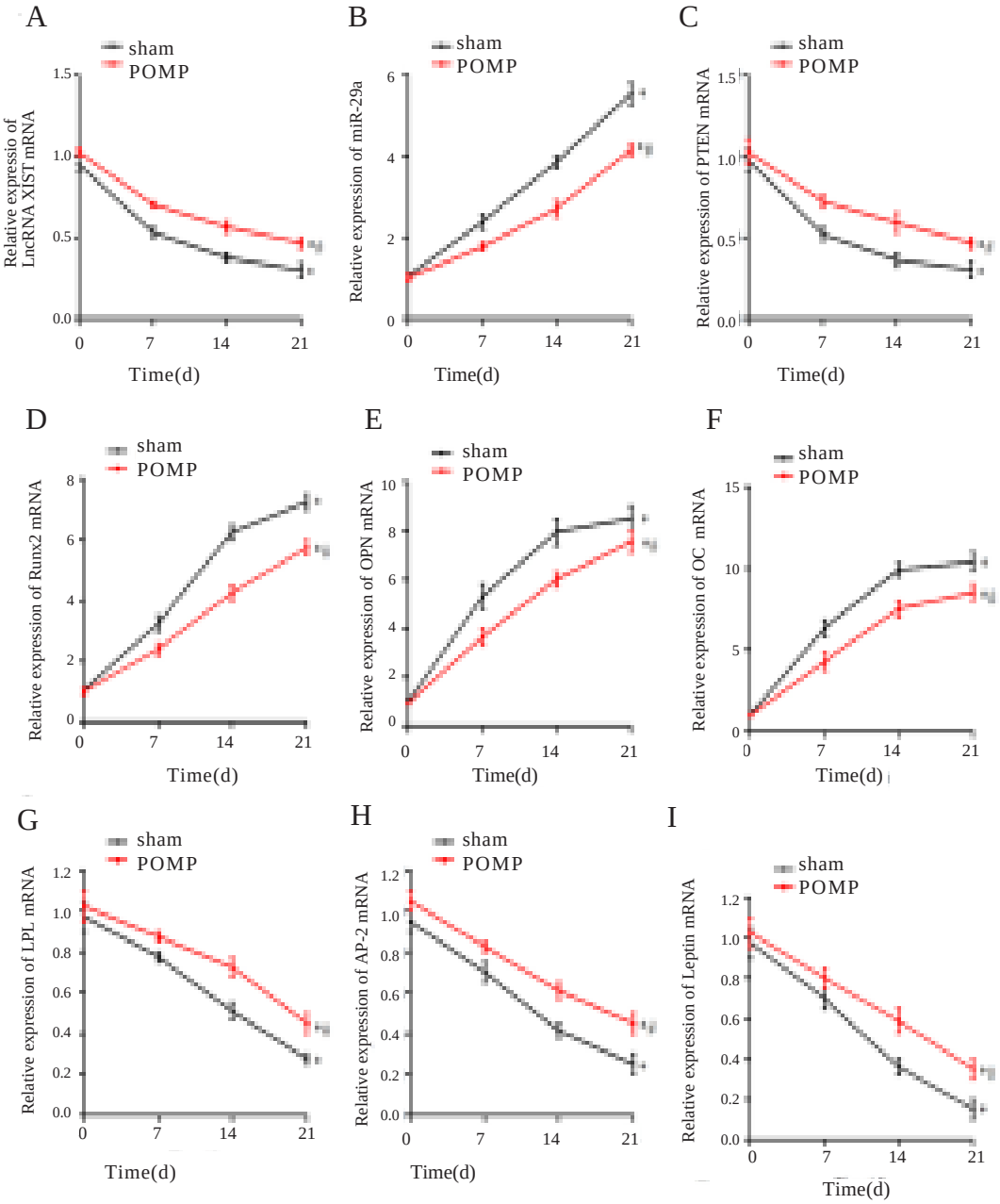

Fig. 2. MRNA expression levels of lncRNA-XIST, miR-29a, PTEN, osteogenic markers Runx2, OPN and OCN and adipogenic markers LPL, AP-2 and leptin during osteogenic differentiation of BMSCs. A) LncRNA-XIST mRNA level; B) miR-29a level; C) PTEN mRNA level; D) Runx2 mRNA level; E) OPN mRNA level; F) OCN mRNA level; G) LPL mRNA level; H) AP-2 mRNA level; I) Leptin mRNA level. *P<0.05 *vs.* 0 d, #P<0.05 *vs.* Sham group

assay, miR-29a significantly down-regulated the expressions of wild-type lncRNA-XIST and PTEN ($P<0.05$), but hardly affected those of mutant lncRNA-XIST and PTEN, indicating targeted regulatory relationships among lncRNA-XIST, miR-29a and PTEN (Fig. 3B and 3D). Meanwhile, the mRNA expression levels of miR-29a, lncRNA-XIST and PTEN were detected using qRT-PCR (Fig. 3E), and Western blotting was used to detect the protein levels of XIST and PTEN (Fig. 3F). Compared to the miR-NC + Lenti-NC group, increased mRNA and protein expressions of lncRNA-XIST and PTEN, but a downward expression of miR-29a in miR-NC + Lenti-XIST and miR-NC + Lenti-PTEN groups ($P<0.05$). Moreover, miR-29a + Lenti-NC group exhibited declined mRNA and protein expressions of lncRNA-XIST and PTEN but elevated miR-29a content ($P<0.05$). In contrast to the miR-29a + Lenti-NC group, miR-29a + Lenti-XIST and miR-29a + Lenti-PTEN groups had increased mRNA and protein expressions of lncRNA-XIST and PTEN, but a downward expression of miR-29a ($P<0.05$). Collectively, the levels of lncRNA-XIST, miR-29a and PTEN interacted with each other.

Differentiation of BMSCs into Osteocytes

To assess the differentiation of BMSCs into osteocytes, osteogenic markers were detected by ALP staining, alizarin red staining, qRT-PCR and Western blotting. It was uncovered in ALP stain-

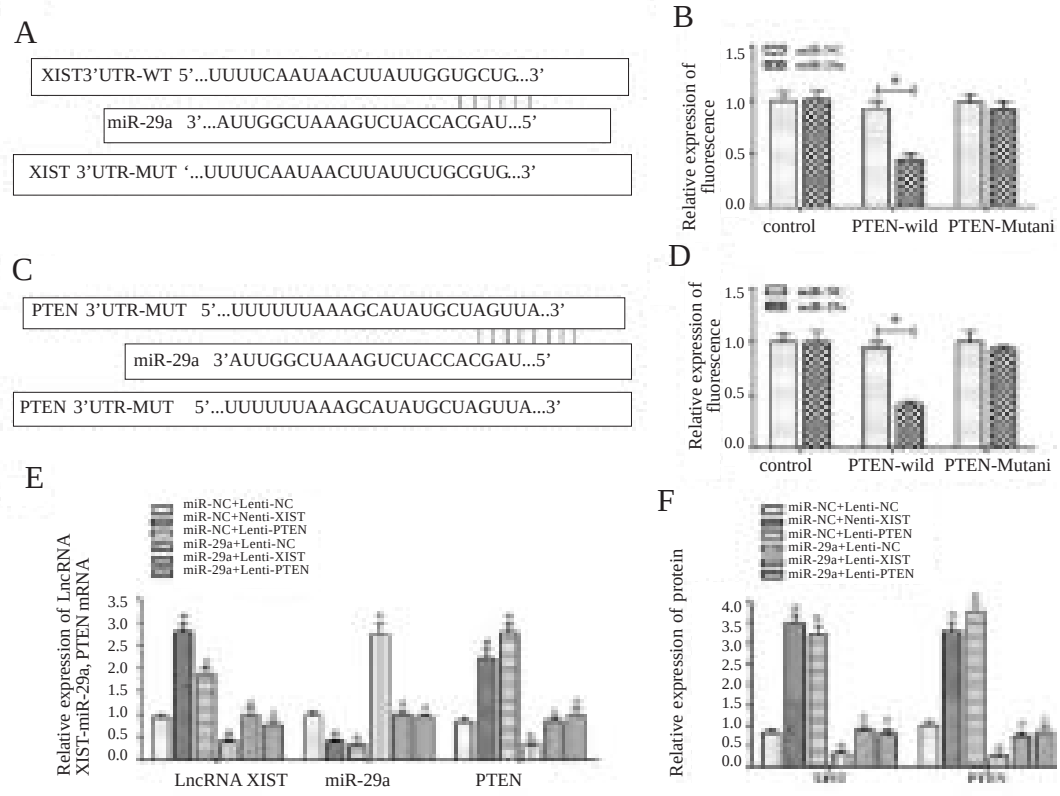

Fig. 3. Targeted regulatory relationships among lncRNA-XIST, miR-29a and PTEN. A) Binding between lncRNA-XIST and miR-29a; B) luciferase assay showed that miR-29a was the target of lncRNA-XIST; C) binding between PTEN and miR-29a; D) luciferase assay showed that PTEN was the target of miR-29a; E) OPN mRNA level; F) OCN mRNA level. *P<0.05 *vs.* miR-NC + Lenti-NC group, #P<0.05 *vs.* miR-29a + Lenti-NC group

ing (Fig. 4A) that in contrast with the miR-NC + Lenti-NC group, miR-NC + Lenti-XIST and miR-NC + Lenti-PTEN groups had significantly fewer blue-purple-stained nodules, and decreased ALP activity (P<0.05). In addition, miR-29a + Lenti-NC group had significantly increased bluish-purple nodules, and enhanced ALP activity (P<0.05). In contrast to the miR-29a + Lenti-NC group, miR-29a + Lenti-XIST and miR-29a + Lenti-PTEN groups had significantly fewer bluish-purple nodules, and decreased ALP activity (P<0.05). Besides, according to alizarin red staining (Fig. 4B), compared with the miR-NC + Lenti-NC group, miR-NC + Lenti-XIST and miR-NC + Lenti-PTEN groups had significantly fewer red calcified nodules, and decreased alizarin red concentration (P<0.05). The miR-29a + Lenti-NC group displayed significantly increased red calcified nodules, and enhanced alizarin red concentration (P<0.05). Compared to the miR-29a + Lenti-NC group, miR-29a + Lenti-XIST and miR-29a + Lenti-PTEN groups had significantly fewer red calcified nodules, and reduced alizarin red concentration (P<0.05). According to qRT-PCR (Fig. 4C) and Western blotting (Fig. 4D), miR-NC + Lenti-XIST and miR-NC + Lenti-PTEN groups exhibited significantly lower mRNA and protein expression levels of Runx2, OPN and OCN than the miR-NC + Lenti-NC group (P<0.05). Additionally, the Runx2, OPN and OCN mRNA and protein expres-

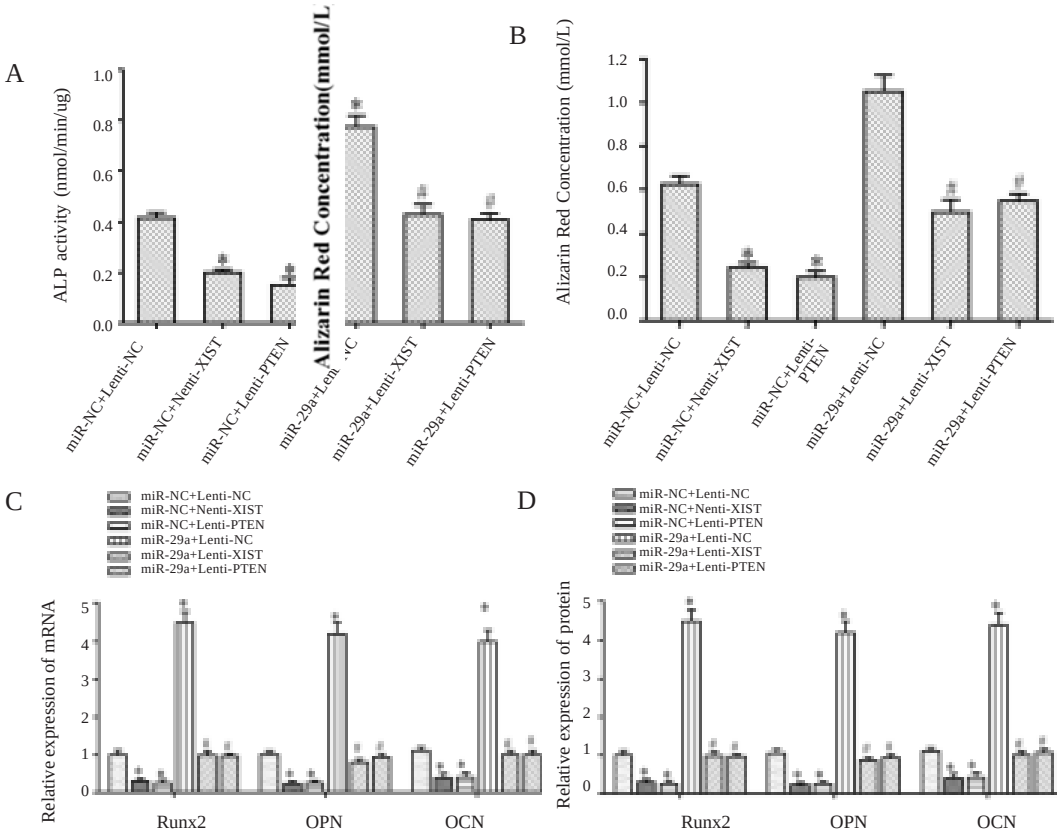

Fig. 4. Differentiation of BMSCs into osteocytes. A) ALP staining (×100); B) alizarin red staining (×100); C) mRNA levels of osteogenic markers ascertained by dint of qRT-PCR; D) protein content of osteogenic markers detected by Western blotting. *P<0.05 *vs.* miR-NC + Lenti-NC group, #P<0.05 *vs.* miR-29a + Lenti-NC group

sion levels significantly rose in the miR-29a + Lenti-NC group (P<0.05). Compared with those in miR-29a + Lenti-NC group, Runx2, OPN and OCN mRNA and protein expression levels significantly declined in miR-29a + Lenti-XIST and miR-29a + Lenti-PTEN groups (P<0.05). In short, miR-29a promoted the early and late osteogenic phenotype transformation of BMSCs and elevated the levels of osteogenic markers, and lncRNA-XIST and PTEN inhibited the differentiation of BMSCs into osteocytes through targeting miR-29a.

Differentiation of BMSCs into Adipocytes

To assess the differentiation of BMSCs into adipocytes, adipogenic markers were ascertained by means of qRT-PCR and Western blotting. According to qRT-PCR (Fig. 5A) and Western blotting (Fig. 5B), the LPL, AP-2 and leptin mRNA and protein expression levels were significantly higher in miR-NC + Lenti-XIST and miR-NC + Lenti-PTEN groups than those in the miR-NC + Lenti-NC group (P<0.05). Moreover, the LPL, AP-2 and leptin mRNA and protein expression levels significantly declined in the miR-29a + Lenti-NC group (P<0.05). In comparison to those in miR-29a + Lenti-NC group, the LPL, AP-2 and leptin mRNA and protein expression levels significantly rose in miR-29a + Lenti-XIST and miR-29a + Lenti-PTEN groups (P<0.05). Overall, miR-29a suppressed the increase in adipogenic markers, and lncRNA-XIST and PTEN enhanced the adipogenic differentiation of BMSCs through targeting miR-29a.

Mechanism of lncRNA-XIST/miR-29a/PTEN Pathway in PMOP

The ovariectomized rat model was established, from which BMSCs were extracted. The expressions of lncRNA-XIST and PTEN in BMSCs were up-regulated, while that of miR-29a was down-regulated, and there were targeted regulatory relationships among lncRNA-XIST, miR-29a and PTEN. Moreover, the osteogenic and adipogenic markers in BMSCs were detected. The overexpression of lncRNA-XIST and PTEN facilitated the expressions of adipogenic markers LPL, AP-2 and leptin but inhibited those of osteogenic markers (Runx2, OPN and OCN), whereas such facilitation and inhibition were reversed following overexpression of miR-29a. The researchers thus postulated that lncRNA-XIST suppressed the differentiation of BMSCs into osteocytes by means of the miR-29a/PTEN pathway (Fig. 6).

DISCUSSION

PMOP is primarily characterized by the devastation of bone microstructure, decline in BMD and increment in bone fragility, which leads to fractures (Watts 2018). In PMOP patients, bone resorption is greater than bone formation, and BMSCs are more prone to adipogenic differentiation. BMSCs are the source of cells for bone regeneration, and their ability of osteogenic differentiation is attenuated with increasing age and degree of osteoporosis (Luo et al. 2019). There-

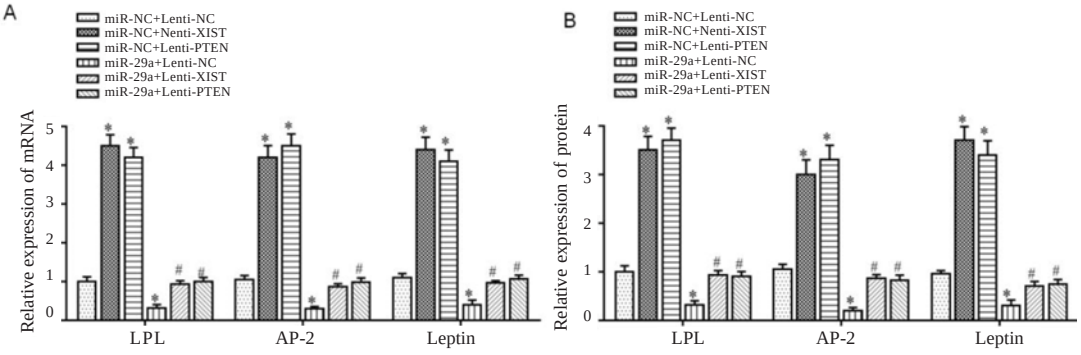

Fig. 5. Differentiation of BMSCs into adipocytes. A) mRNA levels of adipogenic markers ascertained by dint of qRT-PCR; B) protein content of adipogenic markers ascertained by dint of Western blotting. #P<0.05 *vs.* miR-29a+Lenti-NC group

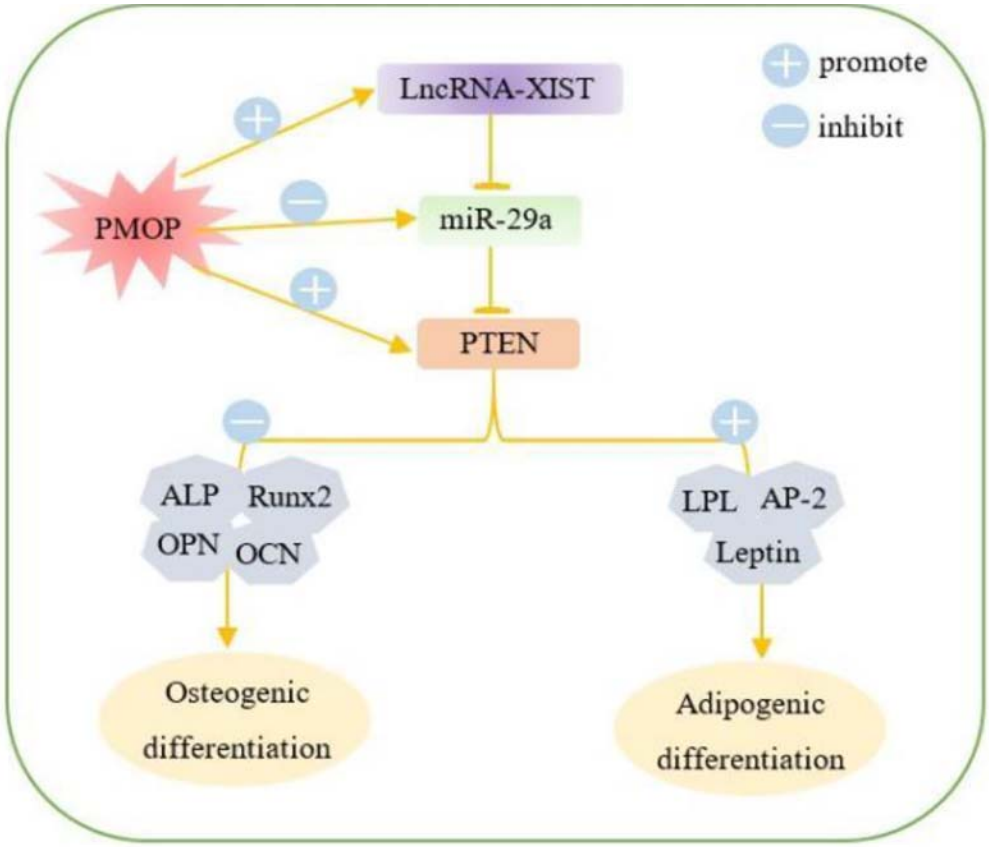

Fig. 6. Mechanism of lncRNA-XIST/miR-29a/PTEN pathway in PMOP

fore, PMOP can be effectively treated by inducing the differentiation of BMSCs into osteocytes (Aghebati et al. 2019).

The important function of lncRNAs in regulating osteoarthritis and osteoporosis has been verified (Zhang et al. 2019; Yang et al. 2020). LncRNA-XIST can enhance osteoblast apoptosis and aggravate iron accumulation-induced osteoporosis in mice (Liu et al. 2021). Moreover, lncRNA-XIST has elevated expression in chondrocytes upon IL-1β-induced osteoarthritis, impedes the proliferation and boosts the apoptosis of chondrocytes (Sun et al. 2020). Consistently, lncRNA-XIST had raised expression in PMOP rats herein, and repressed the differentiation of BMSCs into osteocytes. In addition, miRNAs have been involved in osteoblast and osteoclast differentiation (Fu et al. 2019). For instance, miR-29a boosts the differentiation of MSCs into osteocytes by targeting histone deacetylase 4 (Tan et al. 2018), and targets the receptor activator of nuclear factor-κB ligand to facilitate osteoclast differentiation, thereby protecting bone tissues against osteoporosis (Lian et al. 2019). Notably, the interaction between lncRNAs and miRNAs is implicated in osteogenic differentiation. For instance, as evidenced by study of Zhang et al. (2021), lncRNA-XIST displayed a raised expression in patients with long-term nonunion, and XIST knockdown induced the osteoblast (MC3T3-E1 cells for example) differentiation through sponging miR-135, thus promoting fracture heal-

ing. LncRNA-XIST weakens the differentiation of BMSCs into osteocytes through suppressing miR-29b-3p and the expressions of ALP and Runx2 in BMSCs, thereby worsening osteoporosis (Yu et al. 2021). In this work, miR-29a expression declined in BMSCs in PMOP rats, and there was a targeted regulatory relationship between miR-29a and lncRNA-XIST. LncRNA-XIST brought down the expression of miR-29a to impede the differentiation of BMSCs into osteocytes. It has been reported that PTEN can inhibit BMP9-induced differentiation of MSCs into osteocytes (Li et al. 2021), and both bone volume and BMD can be greatly boosted by means of the deletion of PTEN (Jin et al. 2020). Many miRNAs have also been involved in PTEN-regulated osteogenic differentiation. For example, miR-29b-3p enhances the differentiation of adipose-derived mesenchymal stem cells into osteocytes by dint of directing PTEN (Xia et al. 2020). MiR-21 facilitates the migration and osteogenic differentiation of BMSCs *in vitro*, consequently advancing maxillofacial bone regeneration (Geng et al. 2020). In this study, the expression of PTEN increased in BMSCs of PMOP rats, and miR-29a advanced the differentiation of BMSCs into osteocytes through targeting PTEN.

There is an inverse proportion between cancellous bone mass and adipocytes in patients with osteoporosis, and excessive adipogenic differentiation is one of the major causes for PMOP (Geng et al. 2020). ALP is a common index for assessing bone formation and bone turnover (Zhao et al. 2015). Runx2, OPN and OCN player crucial roles in bone metabolic regulation and a variety of bone metabolic diseases including PMOP (Shao et al. 2021). LPL, AP-2 and leptin can enhance adipogenesis and suppress osteogenic differentiation. The ability of BMSCs to differentiate into osteoblasts is reduced in PMOP mice, but their ability to differentiate into adipocytes is enhanced, thus giving rise to age-related bone loss (Lin et al. 2019). Research of Qiao et al. (2018) also manifested that BMSCs in PMOP patients had weakened osteogenic ability but enhanced adipogenic ability and miR-203 promoted the differentiation of BMSCs into osteocytes by waning the expression of Dickkopf-like protein 1. In this study, Runx2, OPN and OCN levels were lower, while LPL, AP-2 and leptin levels were higher in BMSCs of PMOP rats than those of normal rats, suggesting that BMSCs were prone to adipogenic differentiation. Meanwhile, the overexpression of lncRNA-XIST and PTEN gave rise to increased Runx2, OPN and OCN levels, but decreased LPL, AP-2 and leptin levels, but such effects were inhibited by the overexpression of miR-29a, indicating that lncRNA-XIST weakened the differentiation of BMSCs into osteocytes by dint of the miR-29a/PTEN pathway.

CONCLUSION

To sum up, lncRNA-XIST and PTEN have incremental expressions, whereas miR-29a manifests a downward expression in BMSCs. LncRNA-XIST suppresses the differentiation of BMSCs into osteocytes by dint of the miR-29a/PTEN pathway.

RECOMMENDATIONS

The findings provide a theoretical and experimental basis for exploring the regulatory function of lncRNA-XIST on the differentiation of BMSCs into osteocytes and future application in the treatment of PMOP.

ABBREVIATIONS

ALP: Alkaline phosphatase; AP-2: adipocyte binding protein-2; BMSC: bone marrow mesenchymal stem cell; lncRNA-XIST: long non-coding ribonucleic acid X inactive specific transcript; LPL: lipoprotein lipase; miR-29a: microRNA-29a; OCN: osteocalcin; OPN: osteopontin; PMOP: postmenopausal osteoporosis; PTEN: phosphatase and tensin homolog deleted on chromosome ten; Runx2: Runt-related transcription factor 2.

REFERENCES

Aghebati-Maleki L, Dolati S, Zandi R et al. 2019. Prospect of mesenchymal stem cells in therapy of osteoporosis: A review. *J Cell Physiol,* 234(6): 8570-8578.

Alsina-Sanchís E, García-Ibáñez Y, Figueiredo AM et al. 2018. ALK1 loss results in vascular hyperplasia in mice and humans through PI3K activation. *Arterioscler Thromb Vasc Biol,* 38(5): 1216-1229.

Baccaro LF, Conde DM, Costa-Paiva L et al. 2015. The epidemiology and management of postmenopausal osteoporosis: A viewpoint from Brazil. *Clin Interv Aging,* 10: 583-591.

Fu YC, Zhao SR, Zhu BH et al. 2019. MiRNA-27a-3p promotes osteogenic differentiation of human mesenchymal stem cells through targeting ATF3. *Eur Rev Med Pharmacol Sci,* 23(3 Suppl): 73-80.

Geng Z, Yu Y, Li Z et al. 2020. miR-21 promotes osseointegration and mineralization through enhancing both osteogenic and osteoclastic expression. *Mater Sci Eng C Mater Biol Appl,* 111: 110785.

Ghafouri-Fard S, Abak A, Avval ST et al. 2021. Contribution of miRNAs and lncRNAs in osteogenesis and related disorders. *Biomed Pharmacother*, 142: 111942.

Jin CY, Jia LF, Tang ZH et al. 2020. Long non-coding RNA MIR22HG promotes osteogenic differentiation of bone marrow mesenchymal stem cells via PTEN/AKT pathway. *Cell Death Dis,* 11(7): 601.

Li FS, Li PP, Li L et al. 2021. PTEN reduces BMP9-induced osteogenic differentiation through inhibiting Wnt10b in mesenchymal stem cells. *Front Cell Dev Biol,* 8: 608544.

Lian WS, Ko JY, Chen YS et al. 2019. MicroRNA-29a represses osteoclast formation and protects against osteoporosis by regulating PCAF-mediated RANKL and CXCL12. *Cell Death Dis,* 10(10): 705.

Lin YP, Liao LM, Liu QH et al. 2021. MiRNA-128-3p induces osteogenic differentiation of bone marrow mesenchymal stem cells via activating the Wnt3a signaling. *Eur Rev Med Pharmacol Sci,* 25(3): 1225-1232.

Lin ZY, He HB, Wang M et al. 2019. MicroRNA-130a controls bone marrow mesenchymal stem cell differentiation towards the osteoblastic and adipogenic fate. *Cell Prolif,* 52(6): e12688.

Liu H, Wang YW, Chen WD et al. 2021. Iron accumulation regulates osteoblast apoptosis through lncRNA XIST/miR-758-3p/caspase 3 axis leading to osteoporosis. *IUBMB Life,* 73(2): 432-443.

Luo B, Yang JF, Wang YH et al. 2019. MicroRNA-579-3p promotes the progression of osteoporosis by inhibiting osteogenic differentiation of mesenchymal stem cells through regulating Sirt1. *Eur Rev Med Pharmacol Sci,* 23(16): 6791-6799.

Luo ZW, Liu YW, Rao SS et al. 2019. Aptamer-functionalized exosomes from bone marrow stromal cells target bone to promote bone regeneration. *Nanoscale*, 11(43): 20884-20892.

Qiao L, Liu D, Wang YJ. 2018. MiR-203 is essential for the shift from osteogenic differentiation to adipogenic differentiation of mesenchymal stem cells in postmenopausal osteoporosis. *Eur Rev Med Pharmacol Sci,* 22(18): 5804-5814.

Shao H, Wu R, Cao L et al. 2021. Trelagliptin stimulates osteoblastic differentiation by increasing runt-related transcription factor 2 (RUNX2): A therapeutic implication in osteoporosis. *Bioengineered*, 12(1): 960-968.

Söreskog E, Lindberg I, Kanis JA et al. 2021. Cost-effectiveness of romosozumab for the treatment of postmenopausal women with severe osteoporosis at high risk of fracture in Sweden. *Osteoporos Int,* 32(3): 585-594.

Sun PF, Wu YP, Li XZ et al. 2020. miR-142-5p protects against osteoarthritis through competing with lncRNA XIST. *J Gene Med,* 22(4): e3158.

Sun X, Cao JC, Han JS et al. 2021. Experimental study of lncRNA RP11-815M8.1 Promoting osteogenic differentiation of human bone marrow mesenchymal stem cells. *Biomed Res Int,* 2021: 5512370.

Tan K, Peng YT, Guo P 2018. MiR-29a promotes osteogenic differentiation of mesenchymal stem cells via targeting HDAC4. *Eur Rev Med Pharmacol Sci,* 22(11): 3318-3326.

Wang Z, Ge X, Wang Y et al. 2021. Mechanism of dexmedetomidine regulating osteogenesis-angiogenesis coupling through the miR-361-5p/VEGFA axis in postmenopausal osteoporosis. *Life Sci,* 275: 119273.

Wang ZQ, Xiu DH, Jiang JL et al. 2020. Long non-coding RNA XIST binding to let-7c-5p contributes to rheumatoid arthritis through its effects on proliferation and differentiation of osteoblasts via regulation of STAT3. *J Clin Lab Anal,* 34(11): e23496.

Watts NB. Postmenopausal osteoporosis: A clinical review. *Journal of Women's Health.* 2018, 1;27(9):1093-6.

Xia T, Dong SH, Tian JW 2020. miR 29b promotes the osteogenic differentiation of mesenchymal stem cells derived from human adipose tissue via the PTEN/AKT/â catenin signaling pathway. *Int J Mol Med,* 46(2): 709-717.

Xu X, Zhang P, Li XF et al. 2020. MicroRNA expression profiling in an ovariectomized rat model of postmenopausal osteoporosis before and after estrogen treatment. *Am J Transl Res,* 12(8): 4251-4263.

Yang Y, Wang YJ, Wang F et al. 2020. The roles of miRNA, lncRNA and circRNA in the development of osteoporosis. *Biol Res,* 53(1): 40.

Yu J, Xiao M, Ren GH 2021. Long non-coding RNA XIST promotes osteoporosis by inhibiting the differentiation of bone marrow mesenchymal stem cell by sponging miR-29b-3p that suppresses nicotinamide N-methyltransferase. *Bioengineered,* 12(1): 6057-6069.

Zhang DW, Chen T, Li JX et al. 2021. Circ_0134944 inhibits osteogenesis through miR-127-5p/PDX1/SPHK1 pathway. *Regen Ther,* 18: 391-400.

Zhang Y, Wang FY, Chen GX et al. 2019. LncRNA MALAT1 promotes osteoarthritis by modulating miR-150-5p/AKT3 axis. *Cell Biosci,* 9: 54.

Zhang Y, Yuan Q, Wei Q et al. 2021. Long noncoding RNA XIST modulates microRNA-135/CREB1 axis to influence osteogenic differentiation of osteoblast-like cells in mice with tibial fracture healing. *Hum Cell,* 35(1): 133-149.

Zhao DF, Wang JS, Liu YN et al. 2015. Expressions and clinical significance of serum bone Gla-protein, bone alkaline phosphatase and C-terminal telopeptide of type I collagen in bone metabolism of patients with osteoporosis. *Pak J Med Sci,* 31(1): 91-94.

Zhong W, Li X, Pathak JL et al. 2020. Dicalcium silicate microparticles modulate the differential expression of circRNAs and mRNAs in BMSCs and promote osteogenesis via circ_1983-miR-6931-Gas7 interaction. *Biomater Sci,* 8(13): 3664-3667.

Zhou W, Lin J, Zhao K et al. 2019. Single-cell profiles and clinically useful properties of human mesenchymal stem cells of adipose and bone marrow origin. *Am J Sports Med,* 47(7): 1722-1733.

Zhu Y, Li R, Wen LM 2021. Long non-coding RNA XIST regulates chondrogenic differentiation of synovium-derived mesenchymal stem cells from temporomandibular joint via miR-27b-3p/ADAMTS-5 axis. *Cytokine,* 137: 155352.

Paper received for publication in January, 2022
Paper accepted for publication in May, 2022